Journal of Sciences, Islamic Republic of Iran 33(4): 319 - 331 (2022) http://jsciences.ut.ac.ir
University of Tehran, ISSN 1016-1104

Novel 4-hydroxycoumarin Derivatives Linked to N-benzyl Pyridinium Moiety as Potent Acetylcholinesterase Inhibitors: Design, Synthesis, Biological Evaluation and Docking Study

M. Abdollahi fard[1], M. Motevalian[2*], M. Manafi[1], S. S. Homami[1]

[1] *Department of Applied Chemistry, Faculty of Science, South Tehran Branch, Islamic Azad University, Tehran, Islamic Republic of Iran*
[2] *Pharmacology Department, Medical School & Razi drug research center, Iran University of Medical Sciences, Tehran, Islamic Republic of Iran*

Received: 1 February 2022 / Revised: 30 August 2022 / Accepted: 13 September 2022

Abstract

Based on the important interactions of donepezil with cholinesterase receptor, a series of coumarin-based N-benzyl pyridinium derivatives (**5a-l**) were synthesized and had in-vitro evaluation for their acetylcholinesterase (AChE) and butyrylcholinesterase (BuChE) inhibitory activities. It was revealed that compound **5l** with plausible IC50 values of 0.247 μM and 1.68 μM on AChE and BuChE, respectively was the most potent anticholinesterase inhibitor compared to other synthesized compounds. The enzyme kinetic assay of compound **5l** was conducted on the AChE enzyme and the compound **5l** was found to be a non-competitive inhibitor of the AChE (Ki= 0.356). In addition, the compound **5l** remarkably protected PC12 neurons against H_2O_2-induced cell death. The docking study of compound **5l** revealed that the inhibitor occupied both CAS and PAS binding sites of the AChE enzyme. we have synthesized 12 products in two steps reactions and high to moderate yields. The first step involves the nucleophilic substitution reaction between 4-hydroxycoumarin and pyridyl chloride (3-pyridinium and 4-pyridinium) derivatives, which produces an intermediate of **3**. Following the reaction of this intermediate with benzyl chloride derivatives, led to the synthesis of final products **5**. The results were compared with donepezil and tacrine as standard drugs for AChE and BuChE inhibitory assays. Based on the IC50 values, the tendency to inhibit synthetic compounds in final products for AChE is better than BuChE. Among the products in AChE inhibitory assay, the 3-pyridinium series showed more effectiveness than the 4-pyridinium series. Docking studies and product interactions with cholinesterase receptor active sites clearly show the role of 3-pyridinium derivatives in receptor binding.

Keywords: Coumarin; N-benzyl pyridinium; Donepezil; Acetylcholinesterase; Butyrylcholinesterase.

[*] Corresponding author; Tel: +98-2188622696; Email: motevalian.m@iums.ac.ir

Introduction

Alzheimer's disease (AD) is a neurodegenerative disorder that is characterized by cognitive problems such as learning and memory deficits [1]. The most obvious type of dementia is memory impairment. Memory impairment usually develops gradually and progresses. Memory impairment is initially limited to recent events and lessons learned, but gradually old memories are also damaged [2]. Alzheimer's disease is caused by a variety of factors, mainly due to biochemical abnormalities in protein production, uncontrolled neuronal electrical activity, and changes in the levels of some neurotransmitters. Oxidative stress, increased toxicity associated with increased glutamate levels, decreased acetylcholine levels and inflammation of brain tissue are among the factors involved in the development of this disease. The production of abnormal forms of amyloid-beta peptides and Tau proteins are important precursors of Alzheimer's disease [3].

Due to significant advances in understanding the mechanisms associated with disease progression, effective disease-stopping drugs are still unknown. Current treatments are mostly based on reducing the symptoms of Alzheimer's disease. Today, there is a need for more effective treatments for this disease, and to achieve this goal, a more accurate understanding of the cellular and molecular mechanisms of this disease can help in its timely and effective diagnosis. Clearing different areas of the brain from the presence of amyloid-beta peptides is one of the most important treatments suggested for Alzheimer's. Removal or reduction of amyloid plaques from the hippocampus of Alzheimer's rats has been shown to increase their memory. All drugs approved for the treatment of Alzheimer's disease modulate neurotransmitters such as acetylcholine (ACh) and glutamate. Disease-altering therapies delay the onset of the disease and also slow its progression. Standard drug treatments for Alzheimer's disease include acetylcholinesterase inhibitors and NMDA antagonists. Psychotropic drugs are used to treat secondary Alzheimer's, such as sleep disorders and depression [4, 5]. In vertebrates, two types of enzymes, acetyl and butyrylcholinesterase (AChE and BuChE), are encoded by genes. Although the two enzymes are located on different chromosomes, including chromosome 7 for acetylcholinesterase and chromosome 3 for butyrylcholinesterase, they have 65% similarity in the amino acid sequence. These enzymes belong to the alpha/beta hydrolase family and are divided into true and false cholinesterase based on the difference in substrates, sensitivity to inhibitors, and behavior against the substrate. It has been observed that in Alzheimer's patients, the level of AChE in the hypothalamus and hippocampus decreases, and the level of BuChE increases. In fact, the enzyme BuChE compensates for the decrease in acetylcholinesterase levels and causes the hydrolysis of ACh. Therefore, inhibition of these enzymes can eliminate the symptoms and complications of the disease by regulating the level of ACh in the brain [6]. AChE and BuChE are the therapeutic targets for drugs used to treat myasthenia gravis and glaucoma and to treat the symptoms of Alzheimer's disease-related cholinergic system dysfunction. Some drugs, such as neostigmine, physostigmine, and rivastigmine, are used to treat myasthenia gravis and Alzheimer's by inhibiting the cholinesterase enzymes. Some substances, such as organophosphate pesticides (including parathion) and chemical warfare gases such as diisopropyl fluorophosphate, are also used to inhibit the cholinesterase enzyme.

By identifying the three-dimensional structure of the enzyme acetylcholinesterase, we have increased our knowledge of the structural components required to inhibit the enzyme. Subsequent identification of the structure of human acetylcholinesterase allows us to design its inhibitors based on the structure of the enzyme. In vertebrates, choline esterase can be used as a target for natural and synthetic toxins to treat neuromuscular disorders and the first generation of Alzheimer's drugs. This enzyme is also the target of organophosphate and carbamate insecticides in invertebrates [7, 8]. Also, Many articles have been published on the synthesis and study of cholinesterase and amyloid-β aggregation inhibitors, for the treatment of Alzheimer's [9-12]. The X-ray crystallographic structure of AChE is composed of two main binding sites: the peripheral anionic site (PAS) consisting of Tyr70, ASP72, Tyr121, Trp279, and Tyr334 amino acid residues which are located in the entrance of the gorge, and the catalytic active site (CAS) lies at the gorge bottom [13], including following subunits: the catalytic triad Ser200-His440-Glu327, the anionic substrate (AS) binding site, Trp84, Glu199, and Phe330 amino acid residues, the acyl binding site (ABS) consisting of Phe288- Phe299 [14]. Furthermore, studies have also demonstrated that molecules interact with PAS or with both PAS and CAS, which can also interfere with the pro-aggregation of amyloid-beta [15, 16].

In the past decades, several AChE inhibitors with different chemical scaffolds such as donepezil [17], tacrine [18], rivastigmine [19], and galantamine [20] were synthesized and used in clinical practice for the treatment of mild to moderate AD. Among these

compounds, donepezil interfaces with both CAS and PAS binding site of AChE, in which benzyl piperidinium moieties of donepezil binds to the CAS [21, 22]. In addition, several reports have demonstrated that benzyl pyridinium residue can be effective for the high anticholinesterase activity of synthetic compounds [23, 24].

Coumarins (2H-chromenee-2-one) are a large family of compounds, which can be obtained from both natural and synthetic sources. Coumarins reported to have a broad range of pharmacological properties, including anti-inflammatory [25], anti-tumor [26], hepatoprotective [27], antifungal [28], antimicrobial [29], anti-oxidant [30], anti-diabetic [31], anti-coagulant [32] and antidepressant effects [33]. Recently, some of the coumarins derivatives such as Ensaculin (KA-672 HCl) [34], AP2238 [35], and scopoletin [36] are considered binding motifs for AChE inhibitors.

Coumarins can inhibit AChE by binding to its PAS [37, 38], moreover, coumarin scaffold was used for MAO-B inhibition [39].

Alzheimer's Disease is a disorder that cannot be properly treated with the old "one target–one molecule" approach, due to its multifactorial character. The complexity of these diseases suggests exploiting the simultaneous modulation of more than one target, a concept known also as multitarget-directed ligands (MTDLs). So The design strategy of new compounds is shown in Figure 1: the N-benzyl pyridinium moiety, could inhibit the AChEs through binding to the catalytic active site (CAS) of AChEs, and the coumarin scaffold was used for MAO-B inhibition and due to the aromatic character, it might have potential interaction with the PAS of AChE (Figure 1). Herein, we describe the synthesis and biological activity of new coumarin-based derivatives linked to benzyl pyridinium scaffold as high effective cholinesterase inhibitors (Scheme 1).

The Alzheimer's disease is investigated into three stages including primary, middle, and the late stages. Nowadays, the researchers has drawn this conclusion that the role of acetylcholinesterase is more pivotal in the primary and middle stages, and the higher amount of this enzyme causes the degradation of acetylcholine. In contrast, in the late stage, the level of acetylcholinesterase in some parts of the brain decrease, yet the amount of butyrylcholinesterase is either constant or even in increase. Therefore, designing the compounds with the ability of dual AchE/BuChE inhibition might be helpful for AD treatment with no

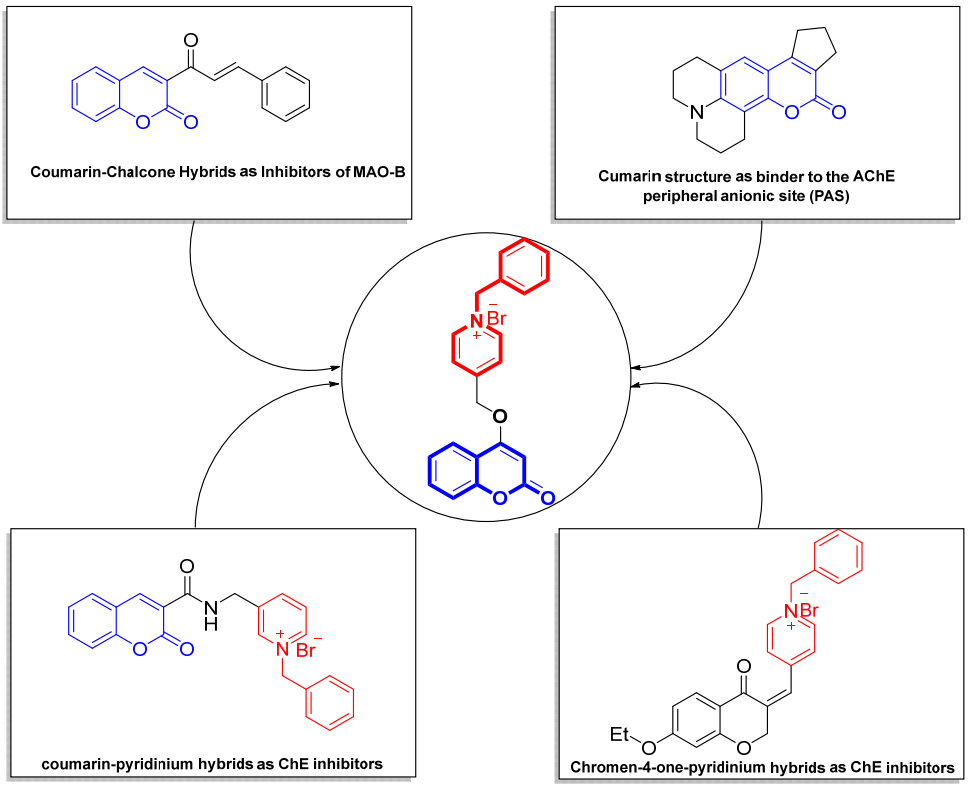

Figure 1. Design strategy of 1-benzyl-3-((2-oxo-2H-chromene-4-yl)oxy)acetamido) methylpyridinium derivatives, including coumarin and pyridinium moieties

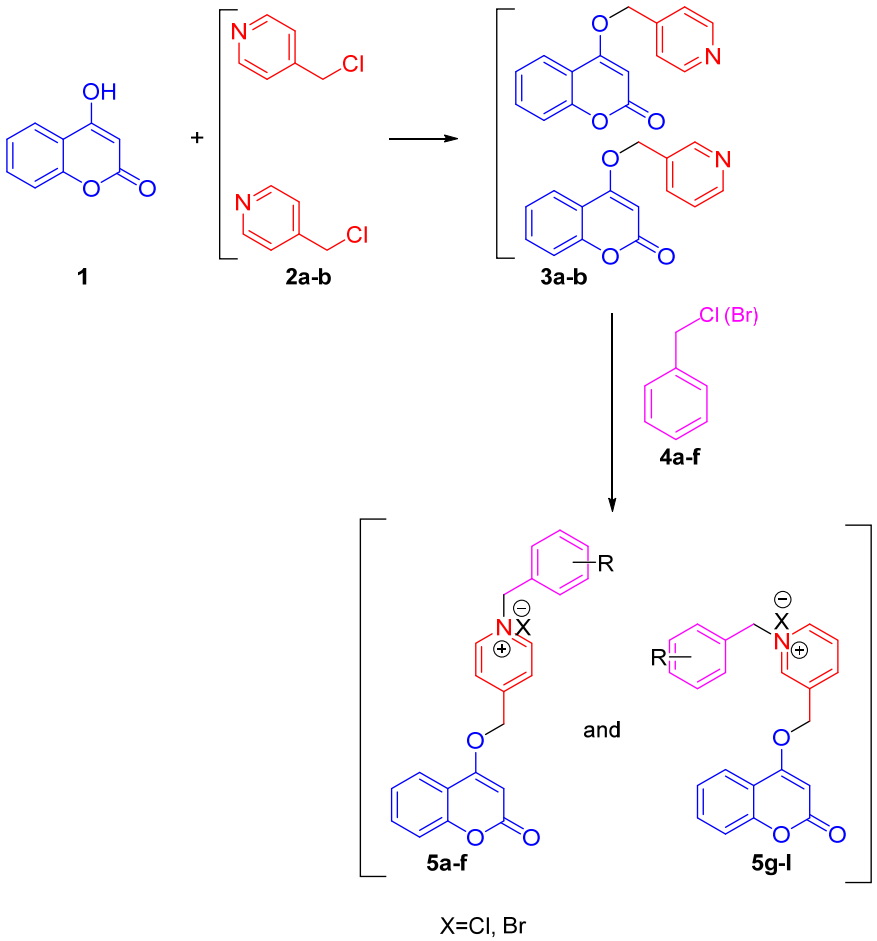

Scheme 1. Synthesis of 7-(pyridin-3 or 4-ylmethoxy)-2H-chromene-2-one derivatives (5a-j)

side effect [21]. On the other hand, the beta-amyloid enzyme interacts through the peripheral anionic site (PAS) and empowers the formation of fibrils. With this information in hand, designing the compounds capable to interact with the enzyme active site as well as he peripheral anionic site (PAS) can be construed as a novel method, and this study has tried to consider all of these factors. The fact that the coumarin core, as mentioned above, has played the primary role and has also been linked to the benzyl PAS core which is in connection with pyridinium through a spacer, can be taken into consideration as the important feature of this compounds. Also, as a final conclusion, it can be stated that the products of this research using a methylene linker have been able to connect the coumarin core and benzylpyridinium as inhibitors of the accumulation of amyloid beta and the double inhibition of AChE/BuChE enzyme , respectively, which in terms of size, as in Figure 2 shows the most fit with the structure of acetylcholine and can be well placed in the active site of the cholinesterase enzyme and cause non-competitive inhibition, which can be attributed to the presence of the coumarin scaffold that has an alpha-beta unsaturated group in its structure. It should also be mentioned that this research led to the introduction of 10 new products with suitable lipophilicity to penetrate the brain by logP range of 1.2315 to 2.4865 (Table 1), which showed good effects against cholinesterase enzymes and especially acetylcholinesterase. It can be used as an alternative treatment for the existing drugs in the early, middle phase of Alzheimer's disease after further and supplementary studies.

Materials and Methods

All starting materials, solvents, and reagents were purchased from commercial suppliers and used without extra purification. All reaction progresses were checked by TLC on Merck silica gel 60 F254 plates and spots were visualized under UV light. The melting points of

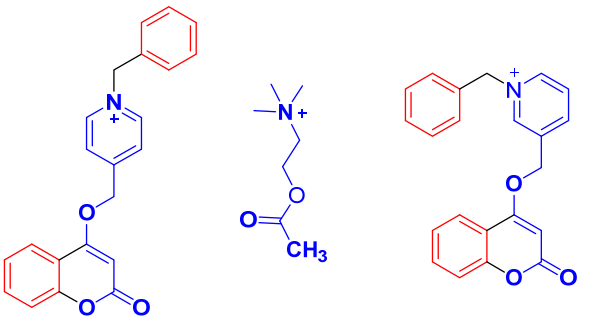

Figure 2. Structural similarity of final products to acetylcholine and the role of phenyl rings (red) in their conversion to cholinesterase inhibitor

Table 1. Inhibition of AChE and BuChE by compounds (5a-l) in comparison with donepezil and tacrine

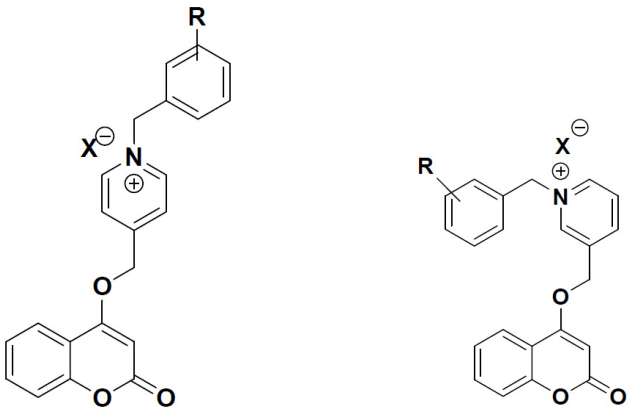

Compounds	X	R	CLogP	IC50(µM) AChE	IC50(µM) BuChE
5a	Cl	4-NO_2	1.2315	2.55	23.46
5b	Br	3-f	1.6315	1.15	13
5c	Br	2-Br	2.3515	1.04	9.05
5d	Br	3-br	2.3515	1.83	6.48
5e	Br	3,5-dimethyl	2.4865	2.16	17.28
5f	Br	3-Cl	2.2015	1.66	9.48
5g	Br	3,5-dimethyl	2.4865	1.29	10.46
5h	Br	2-Me	1.9375	0.512	2.66
5i	Br	2-NO_2	1.2315	0.535	7.92
5j	Cl	4-NO_2	1.2315	0.655	3.5
5k	Br	2-Br	1.3515	0.585	6.43
5l	Br	H	1.4885	0.247	1.68
Donepezil	-	-	3.59759	0.026	0.271
Tacrine	-	-	2.274	0.0318	0.410

[a] Isolated Yield
solvent: ethanol

title compounds were measured by a Kofler hot stage apparatus and were uncorrected. The IR spectra were obtained using Nicolet FT-IR Magna 550 spectrometer (KBr disks). 1H and 13C NMR spectra were recorded

on a Bruker 500 MHz NMR instrument using TMS as an internal standard. The chemical shifts (δ) and coupling constants (J) are expressed in parts per million (ppm) and Hertz (Hz), respectively. Mass spectra were obtained using an Agilent Technology (HP) mass spectrometer operating at an ionization potential of 70 eV. Elemental analysis for C, H, and N has been performed with a PerkinElmer model 240-C apparatus. The results of the elemental analyses (C, H, N) were within ± 0.4% of the calculated values. CLogP (n-octanol/water partition coefficient) has been performed with PerkinElmer ChemDraw Professional version 17.1.

1. General procedure for the preparation of 4-(pyridin-3 or 4-ylmethoxy)-2H-chromene-2-one derivative 3

A mixture of 4-Hydroxycoumarin 1 (1mmol), 3 or 4-(chloromethyl) pyridine 2 (1mmol), and K_2CO_3 in DMF (5ml) was stirred at 80 ºC for 20 h. After completion of the reaction (monitored by TLC), the reaction mixture was allowed to cool at room temperature and poured into crushed ices, and the white precipitates were filtered off. The pure 4-(pyridine-3 or 4-ylmethoxy)-2H-chromene-2-one derivative 3 was recrystallized from EtOH.

2. General procedure for the preparation of 7-(pyridin-3 or 4-ylmethoxy)-2H-chromene-2-one derivatives 5a-l

A solution of benzyl bromide or chloride derivative 4 (1.4 mmol) and the prepared compound 3 was added in dry acetonitrile (10 ml) and heated under reflux condition for 2–3 h. The pure product (5) was filtered off and washed with dry acetonitrile (2 ml)

1-(4-nitrobenzyl)-4-(((2-oxo-2H-chromene-4-yl)oxy)methyl)pyridin-1-ium bromide (**5a**). Yield: 78%; Cream crystals; mp 182-184 ºC. IR (KBR): υ= 3017, 1710, 1619, 1521, 1347 cm^{-1}. ^{1}H-NMR (400 MHz, DMSO-d_6): δH = 9.31 (d, *J*= 6.8 Hz, H-2′, H-6′), 8.34 (d, *J*= 6.4 Hz, H-3′, H-5′), 8.30 (d, *J*= 8.8 Hz, H-3″, H-5″), 8.08 (dd, *J*= 8, 1.2 Hz, H-5), 7.82 (d, *J*= 8.8 Hz, H-2″, H-6″), 7.72 (td, J= 7.8, 1.2 Hz, H-7), 7.46- 7.41 (m, H-6, H8), 6.12 (s, CH_2), 6.04 (s, H-3), 5.78 (s, CH_2) ppm. ^{13}C-NMR (100 MHz, DMSO-d_6): δC = 164.4, 161.7, 155.9, 153.2, 148.3, 145.6, 141.7, 133.6, 130.6, 126.0, 124.8, 124.6, 123.7, 117.0, 115.2, 92.4, 68.6, 62.1 ppm. Anal. Calcd for $C_{22}H_{17}BrN_2O_5$: C, 56.31; H, 3.65; N, 5.97. Found: C, 56.23; H, 3.48; N, 5.71.

1-(3-fluorobenzyl)-4-(((2-oxo-2H-chromene-4-yl)oxy)methyl)pyridin-1-ium bromide (**5b**). Yield: 82%; Cream crystals; mp 200-203 ºC. IR (KBR): υ= 3038, 1721, 1620 cm^{-1}. ^{1}H-NMR (400 MHz, DMSO-d_6): δH = 9.30 (d, *J*= 6.8 Hz, H-2′, H-6′), 8.31 (d, *J*= 6.4 Hz, H-3′, H-5′), 8.07 (dd, *J*= 7.6, 1.2 Hz, H-5), 7.71 (td, *J*= 7.8, 1.2 Hz, H-7), 7.54-7.49 (m, H-6, H8), 7.45-7.40 (m, H-2″, H-5″, H-6″), 7.28 (td, *J*= 8.4, 2.0 Hz, H-4″), 6.03 (s, H-3), 5.97 (s, CH_2), 5.77 (s, CH_2) ppm. ^{13}C-NMR (100 MHz, DMSO-d_6): δ = 164.4, 162.8 (d, *J*= 243.5 Hz), 161.8, 155.7, 153.2, 145.3, 137.1 (d, *J*= 7.8 Hz), 133.6, 131.8 (d, J= 8.4 Hz), 126.0, 125.6 (d, J= 2.8 Hz), 124.8, 123.7, 116.9, 116.7 (d, *J*= 20.7 Hz), 116.4 (d, *J*= 22.4 Hz), 115.3, 92.5, 68.7, 62.4 ppm. Anal. Calcd for $C_{22}H_{17}BrFNO_3$: C, 59.74; H, 3.87; N, 3.17. Found: C, 59.94; H, 3.58; N, 3.33.

1-(2-bromobenzyl)-4-(((2-oxo-2H-chromene-4-yl)oxy)methyl)pyridin-1-ium bromide (**5c**). Yield: 80%; Pink crystals; mp 195-198 ºC. IR (KBR): υ= 2918, 1709, 1619 cm^{-1}. ^{1}H-NMR (400 MHz, DMSO-d_6): δ = 9.10 (d, *J*= 6.8 Hz, H-2′, H-6′), 8.31 (d, *J*= 6.4 Hz, H3′, H-5′), 8.08 (dd, *J*= 7.8, 1.4 Hz, H-5), 7.79 (dd, *J*= 8, 1.2 Hz, H-3″), 7.73 (td, *J*= 7.8, 1.6 Hz, H7), 7.52 (td, J= 7.6, 1.2 Hz, H57.48-7.46 ,(″ (m, H6, H8), 7.43 (dd, J= 7.4, 1.4 Hz, H47.37 ,(″ (dd, J=7.6, 1.2 Hz, H66.05 ;(″(s, H-3), 6.00 (s, CH_2), 5.79 (s, CH_2) ppm. ^{13}C-NMR (100 MHz, DMSO-d_6): δ = 164.4, 161.8, 156.2, 153.3, 145.7, 133.9, 133.6, 133.5, 132.0, 131.8, 129.1, 125.7, 124.8, 123.9, 123.6, 117.0, 115.2, 92.5, 68.6, 63.4 ppm. Anal. Calcd for $C_{22}H_{17}Br_2NO_3$: C, 52.51; H, 3.41; N, 2.87. Found: C, 52.72; H, 3.25; N, 2.64.

1-(3-bromobenzyl)-4-(((2-oxo-2H-chromene-4-yl)oxy)methyl)pyridin-1-ium bromide (**5d**). Yield: 76%; Cream crystals; mp 180-182 ºC. IR (KBR): υ= 3004, 1709, 1618 cm^{-1}. ^{1}H-NMR (400 MHz, DMSO-d_6): δ = 9.12 (d, *J*= 6.8 Hz, H-2′, H-6′), 8.32 (d, J= 6.4 Hz, H-3′, H-5′), 8.09 (dd, *J*= 7.8, 1.4 Hz, H-5), 7.79 (dd, *J*= 3.8, 1.2 Hz, H-4″), 7.72 (td, *J*= 7.8, 1.6, Hz, H-3″), 6.05 Hz, H-7), 7.52 (td, *J*= 7.6, 1.2 Hz, H-2), 7.47-7.42 (m, H-6, H-8, H-6″), 7.46 (td, *J*= 4.6, 1.6 Hz, H-3″), (s, H-3), 6.02 (s, CH_2), 5.79 (s, CH_2) ppm. ^{13}C-NMR (100 MHz, DMSO-d6): δC = 164.3, 161.7, 156.1, 153.2, 145.7, 133.9, 133.6, 133.5, 132.0, 131.9, 129.1, 125.7, 124.8, 123.9, 123.6, 117.0, 115.2, 92.5, 68.6, 63.4 ppm. Anal. Calcd for $C_{22}H_{17}Br_2NO_3$: C, 52.51; H, 3.41; N, 2.87. Found: C, 52.42; H, 3.36; N, 3.04.

1-(3,5-dimethylbenzyl)-3-(((2-oxo-2H-chromene-4-yl)oxy)methyl)pyridin-1-ium bromide (5e). Yield: 74%; White crystals; mp 208-210 ºC. IR (KBR): υ = 3048, 2964, 1715, 1625 cm^{-1}. ^{1}H NMR (500 MHz, DMSO-d^6): δ= 9.22 (d, *J*= 5.2 Hz, H-2′, H-6′), 8.19 (d, *J*= 6.4 Hz, H-3′, H-5′), 8.02 (d, *J*= 7.8 Hz, H-5), 7.71 (t, *J*= 7.8 Hz, H-7), 7.16 (s, H-4″), 7.12 (s, H-2″, H-6″), 7.10 (d, *J*= 7.8 Hz, H-8), 7.05 (m, H-6), 6.34 (s, H-3), 5.79 (s, CH_2), 5.63 (s, CH_2) ppm. ^{13}C-NMR (100 MHz, DMSO-d_6): δ = 160.1, 160.0, 156.5, 155.1, 1144.6, 144.1, 138.4, 134.0, 130.6, 129.7, 126.4, 125.3, 113.1, 112.8, 101.8, 67.4, 62.8 ppm. Anal. Calcd for $C_{24}H_{22}BrNO_3$: C, 63.73; H, 4.90; N, 3.10. Found: C, 63.46; H, 4.71; N, 2.72.

1-(3-bromobenzyl)-4-(((2-oxo-2H-chromene-4-yl)oxy)methyl)pyridin-1-ium bromide (5f). Yield: 82%; Cream crystals; mp 194-196 ºC. IR (KBR): υ= 3026, 2954, 1718, 1622 cm^{-1}. ^{1}H-NMR (400 MHz, DMSO-d6): δ = 9.24 (d, *J*= 6.8 Hz, H-2′, H-6′), 8.20 (d, *J*= 6.4 Hz, H3′, H5′), 8.03 (d, *J*= 8.4 Hz, H-5), 7.71 (d, J= 8.4 Hz, H-4″), 7.51 (dd, *J*= 7.8, 1.6 Hz, H-5), 7.47-7.49 (m, H-8, H-7), 7.40 (d, *J*= 1.6 Hz, H-2), 7.26-7.31 (m, H-6), 7.10-7.13 (m, H-5″, H-6″), 6.35 (s, H-3), 5.90 (s, CH_2), 5.63 (s, CH_2) ppm. ^{13}C-NMR (100 MHz, DMSO-d_6): δ= 164.3, 161.7, 156.1, 153.2, 145.7, 133.9, 133.6, 133.5, 132.0, 131.9, 129.1, 125.7, 124.8, 123.9, 123.6, 117.0, 115.2, 92.5, 68.6, 63.4 ppm. Anal. Calcd for $C_{22}H_{17}BrClNO_3$: C, 57.60; H, 3.74; N, 3.05. Found: C, 79; H, 3.49; N, 3.31.

1-(3,5-dimethylbenzyl)-3-(((2-oxo-2H-chromene-4-yl)oxy)methyl)pyridin-1-ium bromide (5g). Yield: 82%; White crystals; mp 227-229 ºC. IR (KBR): υ = 3020, 2920, 1717, 1618 cm^{-1}. ^{1}H NMR (500 MHz, DMSO-d_6): δ = 9.37 (s, H-6′), 9.26 (*d*, J= 5.8 Hz, H-2′), 8.78 (d, *J*= 8 Hz, H-4′), 8.27 (t, *J*= 7.02 Hz, H-3′), 7.92 (d, *J*= 7.6 Hz, H-5), 7.71 (t, *J*=7.71 Hz, H-7), 7.45 (d, *J*= 8.25 Hz, H-8), 7.40 (t, *J*= 7.5 Hz, H-6), 7.18 (s, H-2″, H-6″), 7.16 (s, H46.08 ,(″ (s, H3), 5.86 (s, CH2), 5.63 (s, CH_2), 2.26 (s, 2× CH_3) ppm. 13C NMR (125 MHz, DMSO-d6): δ =164.0, 161.3, 152.7, 144.7, 144.5, 143.1, 138.4, 136.4, 133.8, 133.0, 130.7, 128.3, 126.5, 124.2, 123.1, 116.5, 114.7, 91.7, 66.8, 63.5, 20.7 ppm. Anal. Calcd for $C_{24}H_{22}BrNO_3$: C, 63.73; H, 4.90; N, 3.10. Found: C, 63.66; H, 4.80; N, 2.98.

1-(2-methylbenzyl)-3-(((2-oxo-2H-chromene-4-yl)oxy)methyl)pyridin-1-ium bromide (5h). Yield: 87%; White crystals; mp 202-205 ºC. IR (KBR): υ= 2996, 2936, 1717, 1622 cm^{-1}. ^{1}H NMR (500 MHz, DMSO-d_6): δ =9.16 (s, H-6′), 9.11 (d, *J*= 6.0 Hz, H-2′), 8.80 (d, *J*= 8.0 Hz, H-6′), 8.28 (t, *J*= 7.0 Hz, H-3′), 7.84 (d, *J*= 7.7 Hz, H-5), 7.71 (t, *J*= 8.0, H-7), 7.45 (d, *J*= 8.3 Hz, H-3″), 7.41 (t, *J*= 7.6 Hz, H-6), 7.15 (d, *J*= 7.1 Hz, H-8), 7.33-7.27 (m, H-4″, H-5″), 7.23 (d, *J*= 7.5 Hz, H-6″), 6.08 (s, H-3), 6.00 (s, CH_2), 5.63 (s, CH_2), 2.30 (s. CH_3). ^{13}C NMR (125 MHz, DMSO-d_6): δ = 163.9, 161.2, 152.7, 144.7, 143.0, 137.1, 136.5, 133.0, 131.9, 130.9, 129.5, 129.4, 128.3, 126.6, 124.2, 123.0, 116.5, 114.7, 91.8, 66.7, 61.7, 18.7 ppm. Anal. Calcd for $C_{23}H_{20}BrNO_3$: C, 63.02; H, 4.60; N, 3.20. Found: C, 63.28; H, 4.81; N, 3.44.

1-(2-nitrobenzyl)-3-(((2-oxo-2H-chromene-4-yl)oxy)methyl)pyridin-1-ium bromide (5i). Yield: 90%; Pale pink crystals; mp 153-155 ºC. IR (KBR): υ = 3023, 1723, 1627, 1524, 1384 cm^{-1}. ^{1}H NMR (500 MHz, DMSO-d_6): δ = 9.26 (s, H-6′), 9.16 (d, *J*= 5.9 Hz, H-2′), 8.86 (d, *J*= 8.0 Hz, H-4′), 8.32 (t, *J*=7.0 Hz, H-3′), 8.24 (d, *J*= 8.1 Hz, H-5), 7.9 (d, *J*= 7.75 Hz, H-3″), 7.84 (t, *J*=7.7 Hz, H-7), 7.44 (d, *J*=7.4Hz, H-6″), 7.40 (t, *J*=7.76 Hz, H-6), 7.32 (d, *J*= 7.6 Hz, H-8), 6.32 (s, CH_2), 6.09 (s, H-3), 5.65(s, CH_2) ppm. ^{13}C NMR (125 MHz, DMSO-d_6): δ = 160.2, 160.0, 157.1, 155.1, 147.5, 145.2, 144.5, 144.1, 134.9, 130.8, 130.6, 129.8, 125.6, 125.3, 124.7, 113.1, 112.8, 111.3, 102.1, 67.5, 60.1 ppm. Anal. Calcd for $C_{22}H_{17}BrN_2O_5$: C, 56.31; H, 3.65; N, 5.97. Found: C, 56.38; H, 3.50; N, 5.84.

1-(4-nitrobenzyl)-3-(((2-oxo-2H-chromene-4-yl)oxy)methyl)pyridin-1-ium bromide (5j). Yield: 80%; Pale pink crystals; mp 201-204 ºC. IR (KBR): υ = 3227, 1712, 1523, 1347 cm^{-1}. ^{1}H NMR (500 MHz, DMSO-d6): δ = 9.42 (s, H-6′), 9.30 (d, *J*= 5.9 Hz, H-2′), 8.83 (d, *J*=8.0 Hz, H-4′), 8.33-8.29 (m, H-3′, H-3″, H-5″), 7.94 (d, *J*= 7.75 Hz, H-5), 7.82 (d, *J*= 8.6 Hz, H-2″, H-6″), 7.70 (t, *J*= 8.3 Hz, H-7), 7.45- 7.39 (m, H-6, H-8), 6.13 (s, CH_2), 6.09 (s, H-3), 5.62 (s, CH_2) ppm. ^{13}C NMR (125 MHz, DMSO-d_6): δ = 164.0, 161.3, 152.7, 147.9, 145.07, 145.01, 143.7, 141.0, 136.6, 133.0, 130.2, 128.5, 124.2, 124.0, 123.2, 116.4, 114.7, 91.8, 66.7, 62.3 ppm. Anal. Calcd for $C_{22}H_{17}BrN_2O_5$: C, 56.31; H, 3.65; N, 5.97. Found: C, 56.45; H, 3.56; N, 6.12.

1-(2-bromobenzyl)-3-(((2-oxo-2H-chromene-4-yl)oxy)methyl)pyridin-1-ium bromide (5k). Yield: 85%; Cream crystals; mp 203-205 ºC. IR (KBR): υ = 2933, 1707, 1620 cm^{-1}. ^{1}H NMR (500 MHz, DMSO-d6): δ = 9.27 (s, H-6′), 9.20 (d, *J*= 5.9 Hz, H-2′), 8.85 (d, *J*= 8.0 Hz, H-4′), 8.32 (t, *J*= 7.05 Hz, H-3′), 7.87 (d, *J*= 7.65 Hz, H-5), 7.76 (d, *J*= 7.85 Hz, H-7), 7.40 (t, *J*=7.45 Hz, H-3″), 7.52-7.47 (m, H-6, H-8), 7.44-7.39 (m, H-4″, H-5″, H-6″), 6.14 (s, CH_2), 6.07 (s, H-3), 5.66 (s, CH_2) ppm. ^{13}C NMR (125 MHz, DMSO-d_6): δ =163.9, 161.2, 152.7, 145.1, 143.4, 136.4, 133.3, 133.0, 132.8, 131.7, 131.6, 128.6, 128.2, 124.2, 123.5, 123.0, 116.4, 114.7, 91.8, 66.7, 63.4 ppm. Anal. Calcd for $C_{22}H_{17}Br_2NO_3$: C, 52.51; H, 3.41; N, 2.87. Found: C, 52.38; H, 3.16; N, 2.76.

1-benzyl-3-(((2-oxo-2H-chromene-4-yl)oxy)methyl)pyridin-1-ium bromide (5l). Yield: 89%; Cream crystals; mp 208-211 ºC. IR (KBR): υ = 3085, 1712, 1625 cm^{-1}. ^{1}H NMR (500 MHz, DMSO-d_6): δ = 9.43 (s, H-6′), 9.30 (d, *J*= 5.7 Hz, H-2′), 8.79 (d, *J*= 7.9 Hz, H-4′), 8.28 (t, *J*=7.0 Hz, H-3′), 7.91 (d, *J*= 7.7 Hz, H-5), 7.70 (t, *J*= 7.5 Hz, H-7), 7.60-7.56 (m, H-6, H-8), 7.50-7.39 (m, H-2″, H-3″, H-4″, H-5″, H6″), 6,08 (s, H-3), 5.95 (s, CH2), 5.63 (s, CH2) ppm. ^{13}C NMR (125 MHz, DMSO-d_6): δ =164.0, 161.3, 152.7, 144.7, 144.6, 143.2, 136.5, 134.1, 133.0, 129.4, 129.1, 128.9, 128.4, 124.2, 123.1, 116.4, 114.7, 91.7, 66.8, 63.4 ppm. Anal. Calcd for $C_{22}H_{18}BrNO_3$: C, 62.28; H, 4.28; N, 3.30. Found: C, 62.54; H, 4.56; N, 3.62.

3. AChE and BChE inhibition assay

Cholinesterase inhibition assay was performed according to the Ellman method. AChE (E.C.3.1.1.7, Type V-S, from Electric eel), BuChE (E.C.3.1.1.8, from equine serum), Ellman's reagent (DTNB), acetylthiocholine (ATC) and butyrylthiocholine (BTC) were obtained from Sigma-Aldrich. Donepezil and tacrine were used as references for ChE inhibition. The reaction took place in a final volume of 3 mL of 0.1 M phosphate buffer, pH 8.0, comprising 50 µl cholinesterase (2.5 IU/ml), 100 µl 5, 5′-dithiobis (2-nitrobenzoic) acid (DTNB) 0.01 M and 20 µl substrate 0.075 M. Inhibition curve was achieved by incubating at least five different concentrations of the tested compound at 25 oC. Absorption was measured by Unico spectrophotometer at 412 nm. Nonlinear regression analysis, using the Graph-Pad Prism program package (GraphPad Software; San Diego, CA), was used to determine IC50 values.

4. AChE enzyme kinetic assay

For the kinetic studies, different concentrations of substrates in the range of 10−3 to 10−10 M and four different concentrations of compound 5l (0, 0.123, 0.247, 0.494 µM) were used, and experiments were conducted at least in triplicate. To determine the type of inhibition of compound 5l, line-weaver-plot was used according to the literature [40].

5. Molecular docking study

Docking studies were performed with Autodock Vina (1.1.2) [41] employing the 3D structure of the AChE enzyme (PDB ID: 1eve) retrieved from Worldwide Protein Data Bank (wwPDB: www.rcsb.org). After removing co-crystallized ligand and water molecules, protein structure was prepared using the Autodock Tools package (1.5.6) [42]. The chemical structure of ligands was sketched using MarvinSketch 5.8.3, 2012, ChemAxon (www.chemaxon.com); then the 2D structures were converted to 3D format by Openbabel (ver 2.3.1) [43] and finally, pdbqt format of ligands was prepared using Autodock Tools python script, prepare_ligand4.py. Docking experiments were performed within a region defined by following parameters: size_x=20, size_y=20, size_z=20, center_x=2.023, center_y=63.295, center_z=67.062. The exhaustiveness was set to 80 and other parameters were left as default. At the end of docking simulations, the best docking solutions were selected for further analysis of enzyme-inhibitor interactions. The graphics are depicted using chimera 1.6 software [44] and PoseView [45].

6. Cellular biology

Cell culture, differentiation, and treatment conditions. PC12 cells were derived from pheochromocytoma of the rat adrenal medulla and cultured in RPMI 1640 medium supplemented with 10 % FCS, 100 units/ml penicillin, and 100 mg/ml streptomycin (All from GIBCO, Grand Island, NY, USA). After trypsinization, the cells were equally seeded into 96-well culture plates (1 × 104 cells/well). The cells were cultured in serum-free medium for 2 days. Afterward, NGF (50 ng/ml, Sigma) was added until neurite outgrowth could be observed [46]. For the neuroprotection assay, firstly non-toxic concentration range of 5l on PC12 cells was determined. Then, PC12 cell differentiation was pretreated with different non-toxic concentrations of 5l (5, 10, and 20 µM) for 3 h. Then, to initiate apoptosis, 350 µl of freshly prepared H_2O_2 was added to the cells and incubated for 24 h. Induction of apoptosis was recognized by DAPI staining.

Measurement of cell viability with MTT assay. After 24 h of incubation, the medium was removed. Cells were washed with PBS and 10 µl of MTT solution (5 mg/ml, Sigma) was added to each well. After 3.5 h of incubation the medium was removed and 150 µl DMSO was added to dissolve formazan precipitates. Finally, optical density (OD) was measured at 560 nm using microplate reader (BioTek Synergy HT) [47]. The viability (%) was calculated as follows:

$$\%\ of\ Viability = \frac{Average\ OD\ of\ treated\ wells - Average\ OD\ of\ blank\ wells}{Average\ OD\ of\ control\ wells - Average\ OD\ of\ blank\ wells} \times 100$$

Results and Discussion

1. Chemistry

The synthetic route for the synthesis of novel series of 4-Hydroxycoumarins linked to N-benzyl pyridinium moieties (5a-l) has been outlined in (Scheme 1). In the first step, 4-(pyridine-3 or 4-ylmethoxy)-2H-chromene-2-one derivatives (3) could be prepared in a convenient way, by the simple reaction of 4-Hydroxycoumarin (1) with 3 or 4-(chloromethyl) pyridine (2) in the presence of K2CO3, in DMF at 100℃. After the completion of the reaction (checked by thin-layer chromatography TLC), the reaction mixture was added to ice water and the precipitate was filtered. The target compounds (5 a-l) were obtained through the N-benzylation of the latter compounds with adequate benzyl bromide or chloride derivatives in acetonitrile under reflux conditions.

Pharmacology (Inhibitory activity against AChE and BuChE)

The cholinesterase inhibitory activity of the synthesized compounds were evaluated according to the Ellman method [48, 49]. The results were compared with the standard drugs (donepezil and tacrine) and evaluated against AChE and BuChE enzymes. The results can be observed as IC50 values in Table 1. The obtained IC50 values of target compounds revealed that several compounds have shown acceptable potency against AChE at concentrations less than 1.00 µM.

Based on the IC50 values for AChE, the inhibitory activity of the 3-pyridinium series (5g-l) were found to be more effective compared to the 4-pyridinium series (5a-f).

In the 3-pyridinium series, compound 5l with no substitution had the highest potency against both enzymes (0.247 µM and 1.68 µM against AChE and BuChE, respectively). Other substitutions' potency has been affected by steric hindrance and electron-inducing properties as the two main factors which decrease their AchE inhibitory activity. Among the substituted derivatives, compound 5f with the methyl group at the ortho-position had a higher potency compared with electron-withdrawing substitutions such as nitro (5i and 5j) and Br (5k). In the 4-pyridinium series, compounds 5a-5f revealed lower potency on both enzymes. Among these series halogen-substituted compounds (5b, 5c, 5d, and 5f) had more affinity against the AChE enzyme compared to the nitro substituted compound (5a) which can be justified by the steric hindrance effect of the nitro group. Overall it can be observed that steric hindrance sensitivity of substitutions based on their anti-AChE efficacy can be expressed in the following order: para> meta> ortho.

The IC50 values of compounds (5a-l) against BuChE were in the range of 1.68 to 23.46 µM, which were notably higher than those of AChE. Among the target compounds, 5l was the best candidate for inhibition of BuChE (IC50 = 1.68 µM).

Enzyme kinetic assay

Enzyme kinetic assay performed on AChE enzyme, to determine the type of inhibition by the most potent compound 5l. As can be seen in (Figure 3-a), the Lineweaver-Burk plot suggested that compound 5l inhibited the AChE enzyme as a non-competitive inhibitor, as with the increase of the inhibitor concentration the Vmax decreased and the value of Km remained unaffected. The secondary replotting of Lineweaver-Burk plots was used to calculate the Ki value of compound 5l which was found to be 0.356 (Figure 3-b).

2. Docking study

In an attempt to study the binding mode of synthesized compounds toward the active site of the AChE enzyme, molecular docking simulations were performed using Autodock Vina (1.1.2) software. For this purpose, the most potent compound 5l was subjected to docking studies and the best pose was further analyzed. As shown in Figure 4, the compound is well accommodated in the active site of the enzyme in such a way that phenyl pyridinium moiety is oriented toward the bottom of the active site. In this position, the quaternary nitrogen of the compound binds Tyr334 through π-cation interaction. As reported in the literature, it seems that this positively charged nitrogen plays an important role in the penetration of the ligand into the active site of the enzyme as well as the inhibition process. Additionally, a π- π interaction between the pyridine ring of ligand and Tyr334 more established compound in the mid-gorge enzyme. The phenyl ring of benzyl moiety is also in parallel disposition to Trp84 showing another π- π interaction. It could be concluded that the ligand is well anchored in

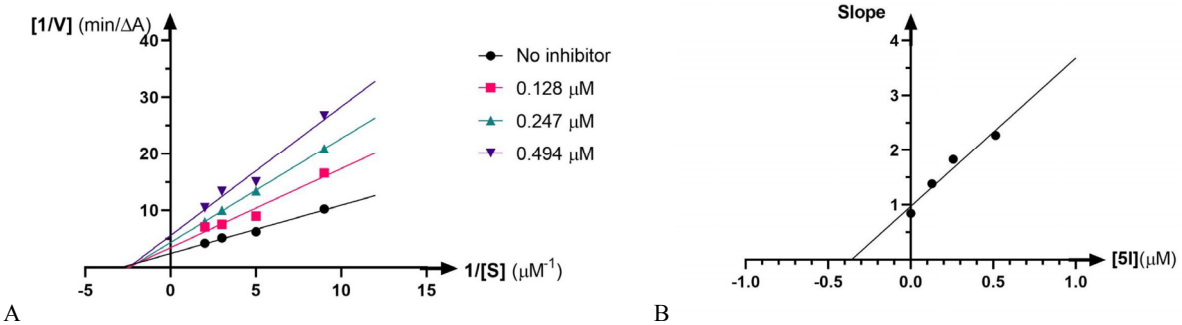

Figure 3. a) Lineweaver-Burk plot as the variation of **1/V** vs. **1/[S]** in the presence of various concentrations of the target compound **5l.** b) Secondary plot as the variation of slope vs. concentration of compound (**5l**).

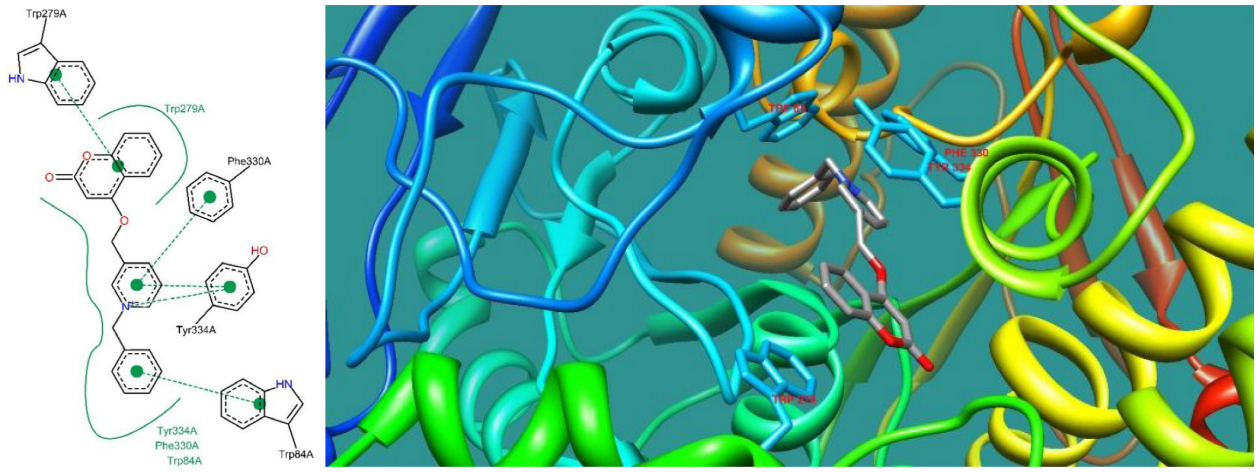

Figure 4. left) 2D representation of compound **5l** interactions with residues in the active site of AChE. right) 3D orientation of **5l** in the active site of the target enzyme.

the mid-gorge of the active site via the aforementioned interactions. Furthermore, the flexibility of the etheric linker allows the coumarin ring to be placed in parallel with Trp279 and binds to it via a π- π interaction.

3. The protective effect of 5g against H_2O_2-Induced cell death

The neuroprotective activity of the compound 5l against H_2O_2-induced cell death in PC12 cell differentiation was investigated. Thus, different concentrations (5, 10, and 20 µM) of the compound 5l were used before Exposure of PC12 cells to H_2O_2. Furthermore, quercetin at the concentration of 5 µM was used as reference compound. Then, to initiate apoptosis, H_2O_2 was added to the cells' medium and incubated for 24 h. Eventually, the induction of apoptosis was recognized by DAPI staining. Cell viability was measured by using the MTT (3-(4,5-dimethylthiazol-2-yl)-2,5-diphenyltetrazolium bromide) assay. As shown in Figure 5, 5l prevents H_2O_2-induced cell death in PC12 cells in a dose-dependentmanner. Accordingly, treatment of PC12 cells with different concentrations of 5l (5-20 µM) for 24 h did not affect the cell viability. While pretreatment of cells with various concentrations of 5l followed by exposure to H_2O_2changed the cell viability. The neuroprotective activity of 5l on cell death occured dose-dependently. Increasing the dose of 5l defused H_2O_2-induced cell death significantly.

Conclusion

A novel series of coumarin-based N-benzyl pyridinium derivatives have been designed and synthesized. In the second step, AChE and BuChE inhibitory actions have been evaluated. The 3-picolyl benzyl derivative showed the most potent anti-AChE and anti-BuChE activity (IC50 values = 0.247 µM and 1.68 µM, respectively). The docking study of compound 5l with AChE enzyme demonstrated that the two distinct regions in the active site of AChE, the catalytic site, and the peripheral anionic site, interact with the ligand. These obtained results make the compound 5l a

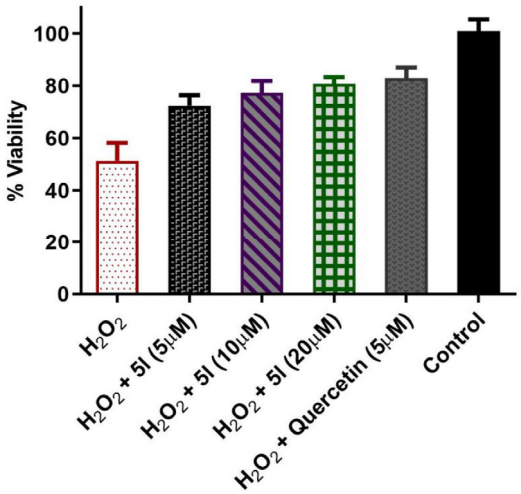

Figure 5. Neuroprotective activity of 5l against H_2O_2-induced cell death in PC12 cells. Dose-dependent protective effect of **5l** on H_2O_2-induced cytotoxicity in PC12 cells. Results represent mean ± SD (n = 3) for each concentration. In each series labeled mean values are significantly different (at $p < 0.001$) according to the H_2O_2 group.

significant cholinesterase inhibitor for subsequent developments and have been revealed using the importance of the 4-Hydroxycoumarin and benzyl pyridinium structures for the further developments of potential multifunctional candidates against AD.

Declaration of conflicting interests

The authors confirm that this article's content has no conflict of interest.

Acknowledgments

The authors appreciate Islamic Azad University, South Tehran Branch for providing grant.

References

1. Eikelenboom P, Zhan SS, van Gool WA, Allsop D. Inflammatory mechanisms in Alzheimer's disease. TIPS. 1994; 15(12): 447-450.
2. Terry AV, Buccafusco JJ. The cholinergic hypothesis of age and Alzheimer's disease-related cognitive deficits: recent challenges and their implications for novel drug development, J. Pharmacol. Exp. Ther. 2003; 306(3): 821-827.
3. Schelterns P, Feldman H. Treatment of Alzheimer's disease; current status and new perspectives. Lancet Neurol. 2003; 2(9): 539-547.
4. Akram M, Nawaz A. Effects of medicinal plants on Alzheimer's disease and memory deficits. Neural Regen. Res. 2017; 12(4): 660.
5. Giacobini E. Cholinesterase inhibitors: new roles and therapeutic alternatives. Pharmacol. Res. 2004; 50(4): 433-440.
6. Decker M, Krauth F, Lehmann J. Novel tricyclic quinazolinimines and related tetracyclic nitrogen bridgehead compounds as cholinesterase inhibitors with selectivity towards butyrylcholinesterase. Bioorg. Med. Chem. 2006; 14(6): 1966-1977.
7. Shan WJ, Huang L, Zhou Q, Meng FC, Li XS. Synthesis, biological evaluation of 9-N-substituted berberine derivatives as multi-functional agents of antioxidant, inhibitors of acetylcholinesterase, butyrylcholinesterase and amyloid-β aggregation, ur. J. Med. Chem. 2011; 46(12): 5885-93.
8. Lane RM, Steven GP, Enz A. Targeting acetylcholinesterase and butyrylcholinesterase in dementia, Int. J. Neuropsychopharmacol. 2006; 9 (1): 101-124.
9. Osborn GG, Saunders AV. Current treatments for patients with Alzheimer disease, Int J Osteopath Med . 2010; 110(98): 16-26.
10. Dinamarca MC, Weinstein D, Monasterio O, Inestrosa NC. The synaptic protein neuroligin-1 interacts with the amyloid β-peptide. Is there a role in Alzheimer's disease?. Biochemistry. 2011; 50(38): 8127-8137.
11. Pera M, Martinez-Otero A, Colombo L, Salmona M, Ruiz-Molina D, Badia A, Clos MV. Acetylcholinesterase as an amyloid enhancing factor in PrP82-146 aggregation process, Mol. Cell. Neurosci. 2009; 40(2): 217-224.
12. Castro A, Martinez A. Peripheral and dual binding site acetylcholinesterase inhibitors: implications in treatment of Alzheimer's disease. Mini Rev Med Chem. 2001; 1(3): 267-272.
13. Silman I, Sussman JL. Acetylcholinesterase: how is structure related to function? Chem. Biol. Interact. 2008; 175(1-3): 3-10.
14. Zhou X, Wang XB, Wang T, Kong LY. Design, synthesis, and acetylcholinesterase inhibitory activity of novel coumarin analogues. Bioorg. Med. Chem. 2008; 16(17): 8011-8021.
15. Inestrosa NC, Alvarez A, Perez CA, Moreno RD, Vicente M, Linker C, Casanueva OI, Soto C, Garrido J. Acetylcholinesterase accelerates assembly of amyloid-β-peptides into Alzheimer's fibrils: possible role of the peripheral site of the enzyme. Neuron. 1996; 16(4): 881-891.
16. Anand P, Singh B, Singh N. A review on coumarins as acetylcholinesterase inhibitors for Alzheimer's disease, Bioorg. Med. Chem. 2012; 20(3): 1175-1180.
17. Sugimoto H, Ogura H, Arai Y, Iimura Y, Yamanishi Y. Research and development of donepezil hydrochloride, a new type of acetylcholinesterase inhibitor. Jpn. J. Pharmacol. 2002; 89(1): `7-20.
18. Qizilbash N, Birks J, Lopez AJ, Lewington S, Szeto S. Tacrine for Alzheimer's disease (Withdrawn paper. 1999, art. no. CD000202). Cochrane Database Syst Rev. 2005; (1).
19. Agid, Y, Dubois B, Anand R, Gharabawi G. International Rivastigmine Investigators.: Efficacy and tolerability of rivastigmine in patients with dementia of the Alzheimer type, Curr Ther Res Clin Exp. 1998; 59(12): 837-845.
20. Kavanagh S, Gaudig M, Van Baelen B, Adami M, Delgado A, Guzman C, Jedenius E, Schäuble B. Galantamine and behavior in Alzheimer disease: analysis of four trials, Acta Neurol. Scand. 2011; 124(5): 302-308.
21. Alipour M, Khoobi M, Foroumadi A, Nadri H, Moradi A, Sakhteman A, Ghandi M, Shafiee A. Novel coumarin derivatives bearing N-benzyl pyridinium moiety: potent and dual binding site acetylcholinesterase inhibitors, Bioorg. Med. Chem. 2012; 20(24): 7214-7222.
22. Rizzo S, Bartolini M, Ceccarini L, Piazzi, L.; Gobbi, S.; Cavalli, A.; Recanatini, M.; Andrisano, V.; Rampa, A.: Targeting Alzheimer's disease: Novel indanone hybrids bearing a pharmacophoric fragment of AP2238, Bioorg. Med. Chem. 2010; 18(5): 1749-1760.
23. Asadi M, Ebrahimi M, Mohammadi□Khanaposhtani M, Azizian H, Sepehri S, Nadri H, Biglar M, Amanlou M, Larijani B, Mirzazadeh R, Edraki N. Design, Synthesis, Molecular Docking, and Cholinesterase Inhibitory Potential of Phthalimide□Dithiocarbamate Hybrids as New Agents for Treatment of Alzheimer's Disease. Chem. Biodivers. 2019; Nov;16(11):e1900370.
24. Arab S, Sadat□Ebrahimi SE, Mohammadi□Khanaposhtani M, Moradi A, Nadri H, Mahdavi M, Moghimi S, Asadi M, Firoozpour L, Pirali□Hamedani M, Shafiee A. Synthesis and Evaluation of Chroman□4□One Linked to N□Benzyl Pyridinium Derivatives as New Acetylcholinesterase Inhibitors. Arch.

Pharm. 2015 Sep;348(9):643-9,
25. Huang XY, Shan ZJ, Zhai HL, Su L, Zhang XY. Study on the anticancer activity of coumarin derivatives by molecular modeling. Chem Biol Drug Des. 2011; 78(4): 651-658.
26. Bahadır Ö, Çitoğlu GS, Özbek H, Dall'Acqua S, Hošek J, Šmejkal K. Hepatoprotective and TNF-α inhibitory activity of Zosima absinthifolia extracts and coumarin. Fitoterapia. 2011; 82(3): 454-459.
27. Sardari S, Nishibe S, Daneshtalab M. Coumarins, the bioactive structures with antifungal property. Stud. Nat. Prod. Chem. 2000; 23: 335-393.
28. Kawase M, Varu B, Shah A, Motohashi N, Tani S, Saito S, Debnath S, Mahapatra S, Dastidar SG, Chakrabarty AN. Antimicrobial activity of new coumarin derivatives. Arzneimittelforschung. 2001; 51(01): 67-71.
29. Kontogiorgis C, Hadjipavlou-Litina D. Biological evaluation of several coumarin derivatives designed as possible anti-inflammatory/antioxidant agents, J Enzyme Inhib Med Chem. 2003; 18(1): 63-69.
30. Lee SO, Choi SZ, Lee JH, Chung SH, Park SH, Kang HC, Yang EY, Cho HJ, Lee KR. Antidiabetic coumarin and cyclitol compounds from Peucedanum japonicum. Arch. Pharm. Res. 2004; 27(12): 1207-1210.
31. Arora RB, Mathur CN. Relationship between structure and anti□coagulant activity of coumarin derivatives, Br. j. pharmacol. chemother. 1963; 20(1): 29-35.
32. Goplen BP, Linton JH, Bell JM. Dicoumarol studies: iii. determining tolerance limits of contamination in low coumarin sweetclover varieties using a cattle bio-assay. Can. J. Anim. Sci. 1964; 44(1): 76-86.
33. Hoerr R, Noeldner M. Ensaculin (KA□672. HCl): A Multitransmitter Approach to Dementia Treatment. CNS drug reviews. 2002; 8(2): 143-158.
34. Piazzi L, Rampa A, Bisi A, Gobbi S, Belluti F, Cavalli A, Bartolini M, Andrisano V, Valenti P, Recanatini M. 3-(4-{[Benzyl (methyl) amino] methyl} phenyl)-6, 7-dimethoxy-2 H-2-chromeneone (AP2238) Inhibits Both Acetylcholinesterase and Acetylcholinesterase-Induced β-Amyloid Aggregation: A Dual Function Lead for Alzheimer's Disease Therapy, J. Med. Chem. 2003; 46(12): 2279-2282.
35. Mogana R, Teng-Jin K, Wiart C. Anti-inflammatory, anticholinesterase, and antioxidant potential of scopoletin isolated from Canarium patentinervium Miq.(Burseraceae Kunth). eCAM. 2013.
36. Razavi SF, Khoobi M, Nadri H, Sakhteman A, Moradi A, Emami S, Foroumadi A, Shafiee A. Synthesis and evaluation of 4-substituted coumarins as novel acetylcholinesterase inhibitors. Eur. J. Med. Chem. 2013; 64: 252-259.
37. Yusufzai SK, Khan MS, Sulaiman O, Osman H, Lamjin DN. Molecular docking studies of coumarin hybrids as potential acetylcholinesterase, butyrylcholinesterase, monoamine oxidase A/B and β-amyloid inhibitors for Alzheimer's disease. Chem. Cent. J. 2018; 12(1):1-57.
38. Moya-Alvarado G, Yañez O, Morales N, González-González A, Areche C, Núñez MT, Fierro A, García-Beltrán O. Coumarin-chalcone hybrids as inhibitors of MAO-B: Biological activity and in silico studies. Molecules. 2021; 26(9): 2430.
39. de Aquino RAN, Modolo LV, Alves RB, de Fátima Â. Synthesis, kinetic studies and molecular modeling of novel tacrine dimers as cholinesterase inhibitors. Org. Biomol. Chem. 2013; 11(48): 8395-8409.
40. Trott O, Olson AJ. AutoDock Vina: improving the speed and accuracy of docking with a new scoring function, efficient optimization, and multithreading, J. Comput. Chem. 2010; 31(2): 455-461.
41. Sanner MF. Python: a programming language for software integration and development. J Mol Graph Model. 1999; 17(1): 57-61.
42. O'Boyle NM, Banck M, James CA, Morley C, Vandermeersch T, Hutchison GR. Open Babel: An open chemical toolbox. J. Cheminformatics. 2011; 3(1): 1-14.
43. Pettersen EF, Goddard TD, Huang CC, Couch GS, Greenblatt DM, Meng EC, Ferrin TE. UCSF Chimera—a visualization system for exploratory research and analysis, J. Comput. Chem. 2004, 25(13), 1605-1612.
44. Stierand K, Rarey M. From Modeling to Medicinal Chemistry: Automatic Generation of Two□Dimensional Complex Diagrams. ChemMedChem: Chemistry Enabling Drug Discovery. 2007; 2(6): 853-860.
45. Koh SH, Kim SH, Kwon H, Park Y, Kim KS, Song CW, et al. Epigallocatechin gallate protects nerve growth factor differentiated PC12 cells from oxidative-radical-stress-induced apoptosis through its effect on phosphoinositide 3-kinase/Akt and glycogen synthase kinase-3. Mol. Brain Res. 2003; 118(1-2): 2-81.
46. Datki Z, Juhász A, Gálfi M, Soós K, Papp R, Zádori D, Penke B. Method for measuring neurotoxicity of aggregating polypeptides with the MTT assay on differentiated neuroblastoma cells, Brain Res. Bull. 2003; 62(3): 223-229.
47. Asadipour A, Alipour M, Jafari M, Khoobi M, Emami S, Nadri H, et al. Novel coumarin-3-carboxamides bearing N-benzylpiperidine moiety as potent acetylcholinesterase inhibitors, Eur. J. Med. Chem. 2013; 70: 623-630.
48. Ellman GL, Courtney KD, Andres Jr V, Featherstone RM. A new and rapid colorimetric determination of acetylcholinesterase activity. Biochem. Pharmacol. 1961; 7(2): 88-95.
49. Branduardi D, Gervasio FL, Cavalli A, Recanatini M, Parrinello M. The role of the peripheral anionic site and cation− π interactions in the ligand penetration of the human AChE gorge. J. Am. Chem. Soc. 2005; 127(25): 9147-9155.